

Circular cartogram via the elastic beam algorithm originated from cartographic generalization

Zhiwei Wei^{a,b*}, Su Ding^c, Wenjia Xu^{a,b}, Lu Cheng^d, Song Zhang^{a,b}, Yang Wang^{a,b*}

^aKey Laboratory of Network Information System Technology (NIST), Aerospace Information Research Institute, Chinese Academy of Sciences, Beijing 100190, China;

^bThe Aerospace Information Research Institute, Chinese Academic of Sciences, Beijing 100190, China; ^cCollege of Environmental and Resource Science, Zhejiang A & F University, Zhejiang 311300, China; ^dSchool of Resource and Environment Science, Wuhan University, Wuhan 430079, China.

Address for correspondence: Zhiwei Wei. E-mail: 2011301130108@whu.edu.cn

Yang Wang. E-mail: Primular@163.com

Circular cartogram via the elastic beam algorithm originated from cartographic generalization

Abstract: The circular cartogram, also known as the Dorling map, is a widely used tool to visualize statistical data. The circular cartogram represents regions as circles with their sizes in proportion to the statistical values, and these circles are displaced with quality requirements such as no overlaps and contiguity maintenance satisfied. The displacement is a basic operation in cartographic generalization to fulfill map requirements, and many algorithms for map objects' displacements have been introduced. The circles in a circular cartogram can also be considered as map objects. Thus, we develop a new approach by using the elastic beam displacement algorithm in cartographic generalization to displace circles in circular cartogram production. First, the initial circles are generated with their sizes in proportion to the statistical values to avoid huge gaps or overlaps. Second, an elastic beam structure is built as a proximity graph by analyzing the spatial relationships between the circles. Third, the circles violating the quality requirements are considered to have a force on the node of a beam. Fourth, the elastic beam algorithm to achieve global optimization is applied to assign forces for each node to decide the new positions of the circles. Steps 2–4 are repeated until a circular cartogram that satisfies the defined quality requirements is obtained. The evaluation results indicate that the circular cartograms generated by the proposed approach have a higher quality for the maintenance of topology relations, contiguities, and relative relations with smaller displacement distances compared to the existing approaches.

Keywords: Cartogram; Dorling Map; Displacement; Population mapping; Energy minimization.

1. Introduction

An area cartogram is a useful tool for quantitative visualization, which can be traced back to at least 1868 (Tobler, 2004). It represents the statistical data (e.g., population, gross domestic product, presidential election results distribution, etc.) by reshaping the geographic regions (states, countries, etc.) with their size in proportion to the statistical values (Nusrat and Kobourov, 2016). Because size and shape are effective graphic variables for visual perception, the area cartogram can enhance the understanding of

map readers by helping them intuitively recognize the quantity and distribution of data (Inoue, 2011).

Many approaches have been proposed to automate the production of area cartograms. These can be classified into complex shape-based and regular shape-based approaches. In the former approach, the complex shapes of the geographic regions are generated with contiguities and topology relations between regions maintained (Chrisman, 1977; Dougenik et al., 1985; Jackel, 1997; Du and Liu, 1999; Chrisman, 2002; Gastner and Newman, 2004; Wolf, 2005; Sun, 2013a; Sun, 2013b; Gastner et al., 2018; Kronenfeld, 2018; Sun, 2020). Thus, cartograms using complex shapes enable a good understanding of the relations between regions. However, significant distortion of these regions may also occur, and it may be hard for users to distinguish their size differences (Inoue, 2011). In the latter approach, regular shapes are used to reshape the geographic regions, such as circles or rectangles, which are familiar to users and make the size differences easier to perceive (Raisz, 1934; Dorling, 1996; Heilmann et al. 2004; Speckmann et al, 2006; van Kreveld and Speckmann, 2007; Inoue, 2011; Buchin et al., 2012; Tang, 2013). If the relations between regions are also well-considered, the spatial data can be better visualized with cartograms using regular shapes in this sense.

The circle, as one of the simplest shapes, is commonly used in area cartograms known as the circular cartogram or Dorling map (Dorling, 1996). Many JavaScript libraries for data visualization including D3 and Protovis integrate the circular cartogram (Bostock et al., 2011; D3, 2011; Protovis, 2010). The circular cartogram is produced as followed: (1) the initial circles are generated in the centers of their represented regions with their radii assigned in proportion to the statistical values; (2) the circles are displaced to avoid overlaps and maintain the contiguities or topology relations between regions. The circle displacement is the key process of circular cartogram production. An algorithm simulating the orbits of stars and planets (SOSP) and the least-squares adjustment (LSA) are introduced to automate the circle displacement (Dorling, 1996; Inoue, 2011; Tang, 2013). However, the SOSP displaces the circles one by one and will result in local optimization. It also cannot well maintain the topology relations and contiguities between regions. The LSA displaces the circles with global optimization, but it is hard to describe all quality requirements with unified linear functions, and the solutions to which do not always exist. Thus, it is very necessary to develop a new approach to displace the circles in circular cartogram production with all quality requirements satisfied as much as possible in a global

optimization.

Displacement is a basic operation in cartographic generalization, and many displacement algorithms have been developed. The elastic beam algorithm is a powerful one among those algorithms because it can achieve global optimization of map quality requirements based on energy minimization (Bader et al., 2001; Liu et al., 2014). The algorithm models the proximity graph for the map objects as an elastic beam structure, and map objects that violate the map quality requirements are considered to have a force that displaces them. The forces on the proximity graph will stretch and bend the beams, and the deformations of the beams are modeled as energy. The final positions of the map objects are obtained by minimizing the energy. The circles of a cartogram can also be considered as map objects. Furthermore, applying forces in cartogram production is not new, such as cartograms based on the rubber-sheet distortion model (Sun, 2020). The requirements, such as avoidance of overlap or contiguity maintenance, can be modeled as attractive or repulsive forces between circles. Thus, the elastic beam algorithm in cartographic generalization can also be applied for circle displacement in circular cartogram production. Because the elastic beam algorithm achieves the global optimization of the involved quality requirements, it will produce a circular cartogram that can satisfy all quality requirements as much as possible. Furthermore, it may be difficult to obtain a satisfactory result only by circle displacement if overlaps or gaps between circles are very large. Thus, it is also very necessary to avoid large gaps or overlaps between circles in initial circle generation process, then it will be easier to obtain a satisfactory result in later circle displacement.

Motivated by these thoughts, we used the elastic beam algorithm to displace the circles in a circular cartogram production. The initial circles are generated with their sizes assigned by using an alternative directions and reduced steps algorithm to avoid huge overlaps or gaps. The circles are then represented as a proximity graph to establish the global structure and maintain their relations, and the proximity graph is considered as an elastic beam structure. The quality requirements for the circular cartogram are then converted into attractive or repulsive forces on each circle (namely the nodes of the beams). The forces are assigned to each circle to decide their new locations using the elastic beam algorithm iteratively until a satisfactory result is obtained.

2. Related works

2.1 *Quality requirements for circular cartogram*

A circular cartogram needs to satisfy specific quality requirements by considering

the readability, aesthetics, and the odds of misunderstanding the represented information. These requirements are usually developed into constraints to govern its production and are summarized as follows:

(1) Geometry

Shape: The regions are represented as circles (Dorling, 1996);

Size: Circles' radii are assigned in proportion to the statistical values (Dorling, 1995);

(2) Relation

Overlap avoidance: Overlaps between circles need to be avoided (Dorling, 1996);

Topology relation maintenance: The topology relations between the regions need to be maintained as much as possible, mainly the adjacent relations (Inoue, 2011);

Relative relation maintenance: The relative relations between the regions need to be maintained as much as possible, specifically with respect to the relative orientation relations (Inoue, 2011);

(3) Distribution

Contiguity maintenance: The contiguity of regions on the original map should be expressed as much as possible (Dorling, 1996);

Total displacement distance minimization: The displacement distance of circles needs to be minimized (Liu et al., 2014).

The constraints summarized above may conflict with or enhance one another, i.e., circles that are displaced to avoid overlaps will inevitably enlarge the total displacement distance. The constraints in circular cartogram production need to be optimized, i.e., fulfilled as much as possible. Furthermore, these constraints may also have different priorities. For example, overlap avoidance may have a higher priority than topology relation maintenance and contiguity maintenance, because the overlaps must be satisfied to avoid visual clutter, while the topology relations and contiguities need to be satisfied as much as possible.

2.2 Algorithms for circular cartograms

One of the earliest examples of a circular cartogram is the population map in *The Rand McNally World Atlas*, which can be traced back to 1897 (Reyes Nunez, 2014). Within a short time, circular cartograms became widely used in magazines and newspapers to visualize energy consumption, population, etc. These early circular cartograms were mostly produced by hand.

Because the initial circles in a circular cartogram can be easily generated according

to the statistical values, the key process of circular cartogram production is to displace these circles to fulfill the defined quality requirements. Approaches for circular cartogram production have been developed to automate the circle displacement process. Dorling (1996) first introduced a computer program that simulates the orbits of stars and planets to displace circles. Therefore, the circular cartogram is also called a Dorling map. But the circles in his approach are displaced one by one, which will result in local optimization. The topology relations and relative relations between circles are also not well maintained. Inoue (2011) then applied least-squares adjustment for circular cartogram production aiming to achieve a global optimization for the involved quality requirements. He tried to describe all constraints as unified linear functions, and the solution for these functions represents the final locations of all circles. But it is hard to describe all involved constraints as unified linear functions if large quantities of regions or constraints are considered. Solutions for these functions may not always exist. Thus, many JavaScript libraries for data visualization such as D3 (2013) and Protovis (2010) still use Dorling's (1996) approach to integrate the circular map. Furthermore, Tang (2013) applied parallel computing by dividing it into subtasks to speed up the production process.

In summary, Dorling's (1996) approach is still commonly used for circular cartogram production, but it cannot satisfy all quality requirements well. Though some approaches using global optimization are also introduced, they may not always have a satisfactory solution. Thus, it is necessary to develop a new approach that can well consider all quality requirements of a circular cartogram. Furthermore, the initial circles in all the mentioned approaches are just simply generated with their sizes in proportion to statistical values, which may lead to huge overlaps or gaps between circles. A new approach is also required for initial circle generation.

2.3 The elastic beam algorithm

The elastic beam algorithm was first proposed by Bader (2001) based on the principle of energy minimization for building displacement and then developed by Liu et al. (2014). The algorithm models the proximity graph for buildings as an elastic beam structure, in which the proximity graph is constructed according to the spatial relations between buildings. The buildings that violate the map quality requirements are considered to have a force that displaces them. Because the edges in proximity graph are considered as elastic beams, the forces on the proximity graph will stretch and bend the beams. The beams will have forces and moments on their two end nodes, which can

be represented as (f_1^x, f_1^y, M_1) and (f_2^x, f_2^y, M_2) (Fig. 1). Then the two end nodes of a beam are displaced or rotated under the forces and moments; their displaced distances and rotated angles can be represented as $(d_{x1}, d_{y1}, \theta_1)$ and $(d_{x2}, d_{y2}, \theta_2)$ (Fig. 1).

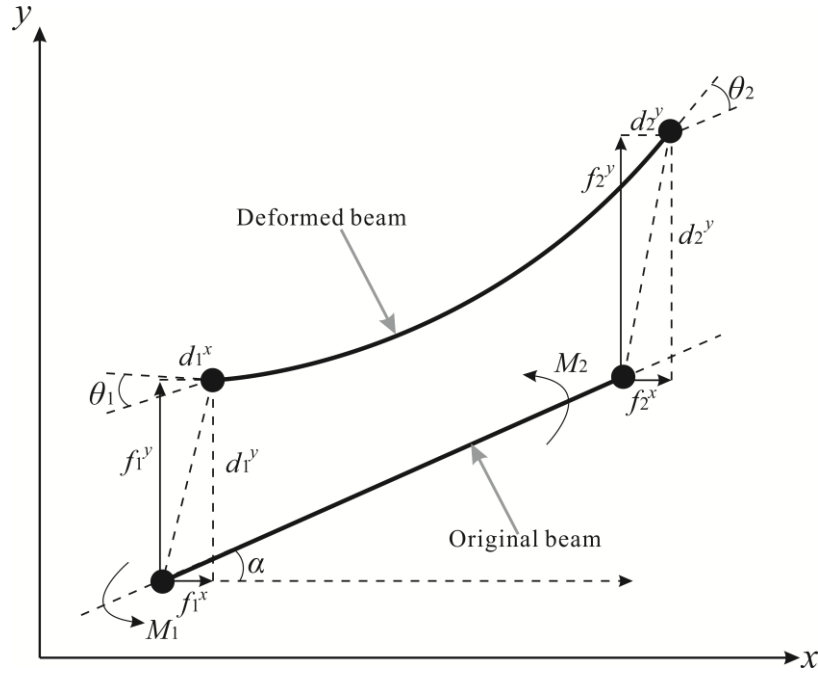


Figure 1. The force analysis of a beam; the figure is based on Liu et al. (2014). (f_1^x, f_1^y, M_1) and (f_2^x, f_2^y, M_2) are the forces and moments applied to the two end nodes of a beam; $(d_{x1}, d_{y1}, \theta_1)$ and $(d_{x2}, d_{y2}, \theta_2)$ are the displaced distances and rotations of the two end nodes of a beam.

The deformations of the beams can be modeled as energy. The optimal shapes and locations of the beams are calculated under the principle of minimum energy, and the buildings' locations after displacement are then obtained. Finite Element Modelling (FEM) was used to solve the minimum energy problem, and the displacement of each building (d) is finally represented as a matrix function [Eq. (1)]; for more details about the mathematical derivation process see Bader (2001) and Liu et al. (2014).

$$d = K^{-1} f \quad (1)$$

where K is the element stiffness matrix of each beam; f is the elemental force of each beam, and the detailed representations for d , K , and f are shown as Eq. (2).

$$\begin{bmatrix} d_{x1} \\ d_{y1} \\ \theta_1 \\ d_{x2} \\ d_{y2} \\ \theta_2 \end{bmatrix} = \frac{l}{E} \begin{bmatrix} Ac^2 + \frac{12I}{l^2}s^2 & (A - \frac{12I}{l^2})cs & -\frac{6I}{l}s & -Ac^2 - \frac{12I}{l^2}s^2 & (A - \frac{12I}{l^2})cs & -\frac{6I}{l}s \\ (A - \frac{12I}{l^2})cs & As^2 + \frac{12I}{l^2}c^2 & \frac{6I}{l}c & -(A - \frac{12I}{l^2})cs & -As^2 - \frac{12I}{l^2}c^2 & \frac{6I}{l}c \\ -\frac{6I}{l}s & \frac{6I}{l}c & 4I & \frac{6I}{l}s & -\frac{6I}{l}c & 2I \\ -Ac^2 - \frac{12I}{l^2}s^2 & -(A - \frac{12I}{l^2})cs & \frac{6I}{l}s & Ac^2 + \frac{12I}{l^2}s^2 & (A - \frac{12I}{l^2})cs & \frac{6I}{l}s \\ -Ac^2 - \frac{12I}{l^2}s^2 & -As^2 + \frac{12I}{l^2}c^2 & -\frac{6I}{l}c & (A - \frac{12I}{l^2})cs & As^2 + \frac{12I}{l^2}c^2 & -\frac{6I}{l}c \\ -\frac{6I}{l}s & \frac{6I}{l}c & 2I & -\frac{6I}{l}s & -\frac{6I}{l}c & 4I \end{bmatrix}^{-1} \begin{bmatrix} f_1^x \\ f_2^y \\ M_1 \\ f_2^x \\ f_2^y \\ M_2 \end{bmatrix} \quad (2)$$

Where A , I , and E are the parameters that describe the material properties of the beams and can be set by users. A controls the stretching and compression property of the beam under axial load, I controls the bending behavior, and E is used to adjust the elasticity of the beams; l is the length of a beam; α is the angle spanned by the beam axis and the x-axis and $s = \sin \alpha$.

3. Methodology

Our approach consists of four steps, as follows.

Step 1: The initial circles are generated according to the statistical values by using an alternative directions and reduced steps algorithm to avoid huge overlaps or gaps;

Step 2: The proximity graph for the circles is built according to the relations of their represented regions;

Step 3: Forces are computed for the proximity graph according to the defined constraints in *Section 2.1*;

Step 4: The forces are assigned for the proximity graph with the elastic beam algorithm to displace the circles. If a result that satisfies the defined constraints in *Section 2.1* is obtained after circle displacement, then stop; otherwise, return to Step 2.

The details for these steps are illustrated in the following sections.

3.1 Step 1: Initial circle generation

The initial circles are generated to represent their corresponding regions with their locations in the centers of the regions, and the radii of the circles are assigned according to the statistical values of the regions. For a region (reg_i) with a value of V_i , the radius (R_i) of the circle that represents reg_i is defined as Eq. (3) (Dorling, 1996).

$$R_i = \sqrt{(V_i - V_{\min}) / (V_{\max} - V_{\min})} * (R_{\max} - R_{\min}) + R_{\min} \quad (3)$$

Where V_{\max} and V_{\min} are the maximum and minimum values of all regions. R_{\min} is the

minimum radius of the circles and can be set based on the minimum resolution of human eyes, e.g., 0.1 mm in graphics (He and Song, 2015). R_{\max} is the maximum radius of the circles, a small R_{\max} will result in great gaps between circles, while a large R_{\max} will result in great overlaps between circles. According to the definition of resolution in a digital elevation model, the R_{\max} is defined according to the average distances between the first 20% of the closest circle pairs ($AveMinD_{20\%}$) with a threshold (T_r) as $(AveMinD_{20\%} - T_r) \leq 0.01\text{mm}$ (Florinsky, 2016). R_{\max} needs to meet the condition $(AveMinD_{20\%} - T_r) \leq 0.01\text{mm}$. This condition is fulfilled by using an alternative directions and reduced steps algorithm, according to Fei (2001). It is a trial-and-error strategy to search a satisfied R_{\max} iteratively, the details of **Algorithm 1** are listed in Table 1.

Table 1. Initial circle generalization using the alternative directions and reduced steps algorithm.

Algorithm 1. Initial circle generalization

Input: The regions, the initial maximum radius of the circles is set as $R_{\max}=50\text{mm}$, the minimum radius of the circles is set as $R_{\min}=0.1\text{mm}$, and the threshold (T_r) is set by users

Output: The initial circles; their locations are in the center of their represented regions, and their radii are assigned according to the statistical values of the regions

Initialize $CacheR_1=R_{\max}$, $CacheR_2=R_{\min}$, $StopLabel=true$

Do

 Compute the initial circles $CS = \{C_1, C_2, \dots, C_m, \dots\}$ with the setting R_{\max} and R_{\min}

 Compute the average distance between the first 20% closest circle pairs ($AveMinD_{20\%}$) for $CS = \{C_1, C_2, \dots, C_m, \dots\}$

If $(AveMinD_{20\%} - T_r) \leq 0.01\text{mm}$ **Then** set $StopLabel=false$

Else If $AveMinD_{20\%} < T_r$ **Then** set $CacheR_1=R_{\max}$, $R_{\max} = (R_{\max} + CacheR_1) / 2$

Else If $AveMinD_{20\%} > T_r$ **Then** set $CacheR_2=R_{\max}$, $R_{\max} = (R_{\max} + CacheR_2) / 2$

While ($StopLabel$)

Return $CS = \{C_1, C_2, \dots, C_m, \dots\}$

3.2 Step 2: Proximity graph construction for the circles

The proximity graph can be constructed considering the spatial relations between the map objects (Wei et al., 2018). As illustrated in Section 2.1, the topology relations and the contiguities between the regions need to be maintained as much as possible. Thus, the initial proximity graph (G) is first constructed for the circles by considering the topology relations between their represented regions.

Suppose the regions as $regS = \{reg_1, reg_2, \dots, reg_m, \dots\}$, the circles representing the regions as $CS = \{C_1, C_2, \dots, C_m, \dots\}$. The proximity graph for CS can be represented as $G = (E, V)$, for which $V = \{v_1, v_2, \dots, v_m\}$ is a node set, v_m represents the circle C_m ; and $E = \{e(v_i, v_j), v_i, v_j \in V\}$ is the edge set. The initial G is built by considering the topology relations and contiguities between the regions as follows: For each two regions reg_i and reg_j in $regS$, if reg_i and reg_j are adjacent to each other, then an edge $e(v_i, v_j)$ connecting their represented circles (C_i and C_j) is inserted in G . The initial G for the regions in Fig. 2(a) can then be built as Fig. 2(b). The length (L) of the $e(v_i, v_j)$ is defined as the distance between its two connected circles (C_i and C_j), given by Eq. (4).

$$L = Dis(C_i, C_j) - (R_i + R_j) \quad (4)$$

$Dis(C_i, C_j)$ is the distance between the centers of C_i and C_j , R_i and R_j are the radii of C_i and C_j . Two refinements are then required by considering the other constraints in Section 2.1 after the construction of the initial G .

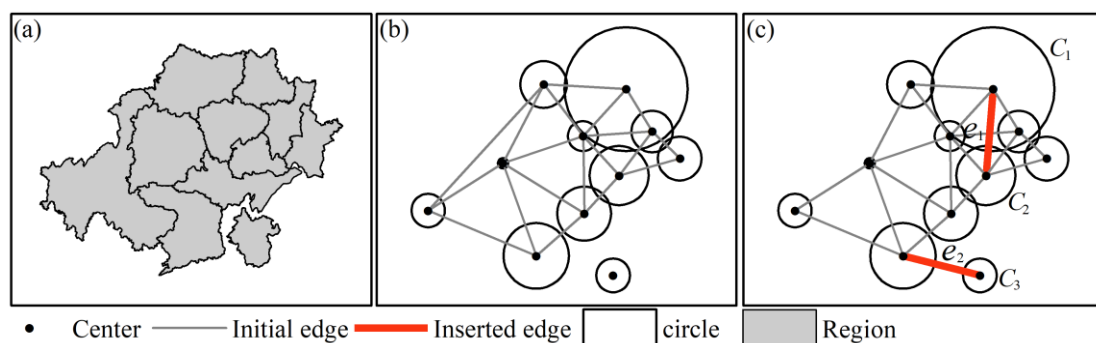


Figure 2. Construction of the proximity graph. (a) The regions; (b) The circles and the built initial proximity graph by considering the topology relations and contiguities between regions; (c) Insert edges by considering avoidance of overlaps and maintenance of relative relations.

(1) Insert edges by considering the avoidance of overlaps

Overlaps of circles need to be avoided in a circular cartogram (Dorling, 1996). But the circles in CS that overlap each other may not all be connected by an edge in the initial G . If any two circles (C_i and C_j) in CS overlap with each other and are not connected by an edge in G , the edge $e(v_i, v_j)$ is then inserted in G . For example, the edge e_1 in Fig. 2(c) is inserted because its connected two circles C_1 and C_2 overlap with each other.

(2) Insert edges by considering the maintenance of relative relations

The relative relations between circles need to be maintained as much as possible (Inoue, 2011). Because we compute the forces for each circle based on the constructed

proximity graph by using the elastic beam algorithm to achieve a global optimization. If all the circles are connected as a group, their displacements will influence one another. Then the structure of the proximity graph can help maintain the relative relations between regions to some extent (Bader, 2001; Liu et al., 2014). But the initial G may have some separate subgraphs and the circles will not be connected as a group, e.g., some of the circles in Fig. 2(b). Suppose G is represented as $G = \{subG_1, subG_2, \dots, subG_n, \dots\}$, where $subG_n$ is a subgraph of G . An edge connecting two nodes in two different $subG$ values with the minimum L is inserted in G until all circles in CS are connected by G as a group. For example, the edge e_2 in Fig. 2(c) connecting C_3 is inserted in G because C_3 is disconnected from any other circles in Fig. 2(c).

(3) Edge classification

After the construction of G , the edges in G can be classified into two types for later force computation by considering the adjacent relations between regions.

- **Type 1:** The edges connecting two circles whose represented regions are adjacent to each other, e.g., the edges in Fig. 2(b);
- **Type 2:** The edges connecting two circles whose represented regions are not adjacent to each other, e.g., e_1, e_2 in Fig. 2(c).

The construction of the proximity graph can be implemented as **Algorithm 2**, described in Table 2.

Table 2. Proximity graph construction algorithm.

Algorithm 2. Proximity graph construction

Input: the regions $regS = \{reg_1, reg_2, \dots, reg_m, \dots\}$, their represented circles $CS = \{C_1, C_2, \dots, C_m, \dots\}$

Output: the proximity graph $G = (E, V)$

Initialize the output proximity graph as $G = (E, V)$, where V is the node set and $V = \{v_1, v_2, \dots, v_m\}$, v_m is the center of the circle C_m ; E is the edge set and $E = Null$

For each node pair $(v_i, v_j), v_i \in V, v_j \in V$ **Do**

If C_i and C_j overlap each other or reg_i and reg_j have an adjacent relation **Then**

add $e(v_i, v_j)$ to E

Group the circles which are connected by an edge in G ; the subgraphs of G are denoted as $G = \{subG_1, subG_2, \dots, subG_n, \dots\}$

While (the subgraphs in G are more than 1) **Do**

Add the edge that connects two nodes separately in two $subGs$ in G with the minimum L

Refresh G

Return $G = (E, V)$

3.3 Step 3: Force computation

Two kinds of forces need to be computed for the proximity graph (G): (1) The two circles connected by an edge in G that have an overlap are repulsed by each other to avoid overlap; and (2) the two separated circles that are connected by a Type 1 edge in G are attracted to each other to maintain the topology relation or contiguity between their represented two regions. A node in G may accept several forces, and these forces need to be combined into a resultant one.

Suppose two circles as C_i and C_j , their radii are R_i and R_j . The edge connecting C_i and C_j is of length L . The centers of C_i and C_j are denoted as O_i and O_j .

(1) Repulsive force

The two circles (C_i and C_j) are repulsed from each other when they have an overlap. The repulsive forces applied for the two circles need to ensure that the overlap can be eliminated. The repulsive force (ref_i and ref_j) for C_i and C_j are defined as Eqs. (5) and (6), and are shown in Fig. 3(a).

$$ref_i = \frac{\overrightarrow{O_j O_i}}{|\overrightarrow{O_i O_j}|} * \frac{R_j}{R_i + R_j} * |L| \quad (5)$$

$$ref_j = \frac{\overrightarrow{O_i O_j}}{|\overrightarrow{O_i O_j}|} * \frac{R_i}{R_i + R_j} * |L| \quad (6)$$

(2) Attractive force

The two separated circles (C_i and C_j) that are connected by a Type 1 edge in G are attracted to each other to maintain the topology relation or contiguity between their represented two regions. The attractive force (atf_i and atf_j) for C_i and C_j are defined as Eqs. (7) and (8), and are shown in Fig. 3(b).

$$rtf_i = \frac{\overrightarrow{O_i O_j}}{|\overrightarrow{O_i O_j}|} * \frac{R_j}{R_i + R_j} * L \quad (7)$$

$$rtf_j = \frac{\overrightarrow{O_j O_i}}{|\overrightarrow{O_i O_j}|} * \frac{R_i}{R_i + R_j} * L \quad (8)$$

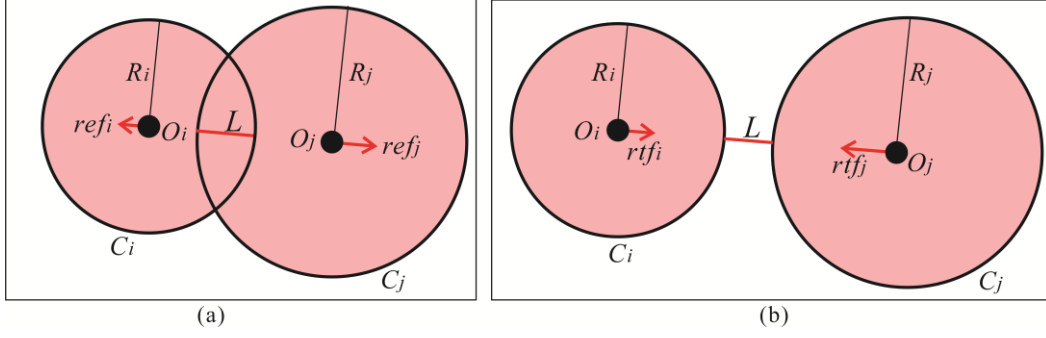


Figure 3. Force computation. (a) Repulsive forces; (b) Attractive forces.

(3) Force combination

A circle may be affected by more than one individual external force (i.e., repulsion or attraction). If these forces are combined into the resultant force by using the simple vector-based summing, inappropriate displacement may occur for the accumulative effect of the forces with a similar direction. Take the circle C_j in Fig. 4(a) as an example, it has two forces f_{ij} and f_{kj} . A coordinate system can be built by taking the direction of f_{ij} as the main direction, and f_{kj} can then be decomposed into two subforces on the x -axis and the y -axis as f_{kj}^x and f_{kj}^y , as shown in Fig. 4(b). If the simple vector-based summing is adopted, the two forces f_{kj}^x and f_{ij} on the x -axis are added together. However, only the larger force (f_{ij}) is needed on the x -axis. Thus, we combine these forces by considering the local maximum component forces in four main directions, e.g., force f_{ij} on the x -axis and f_{kj}^y on the y -axis in Fig. 4(b), and a resultant force can then be obtained. More details about the force combination can be found in Liu et al. (2014).

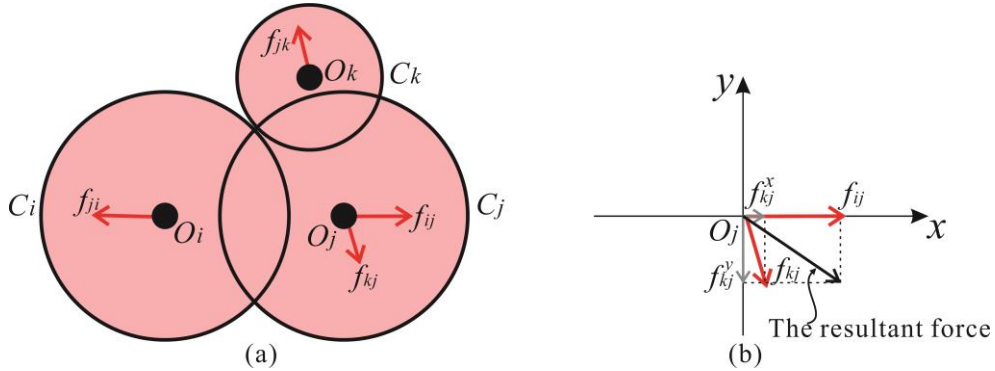


Figure 4. Example for force combination. (a) Forces for each circle; (b) the force combination for circle C_j (Liu et al., 2014).

3.4 Step 4: Using the elastic beam algorithm

The displacement of each node in the proximity graph (G) is computed using the elastic beam algorithm after the construction of G and the computation of the applied forces. Running the algorithm only once cannot guarantee that all conflicts that violate the constraints will be resolved or no new conflicts will arise, particularly in complex

situations (Liu et al., 2014). Thus, an iterative strategy is applied until all circles are in proper locations. All the topology relations or contiguities between regions are constrained to be maintained in the force computation by assigning attractive forces. But the topology relations or contiguities can't all be maintained in practice. Thus, the constraints to maintain topology relations or contiguities between regions will be loosened after a set maximum step (Ts') is reached.

(1) Parameter setting for the elastic beam algorithm

The parameters including E , A , and I need to be set for the elastic beam algorithm as illustrated in *Section 2.3*. Liu et al. (2014) have analyzed the influences of these parameters for displacement results in detail, and the parameters can be set according to their analysis. First, we set $A = L = 1$ to give the beam the same bending and compression properties and reduce the complexity of influencing factors. Second, E_{k+1} is set according to the maximum forces as $\max(f_k)$ for all nodes in the last application of the elastic beam algorithm as follows:

$$E_{k+1} = \frac{\max(d_0)}{\max(f_k)} * E_0 \quad (9)$$

Where $\max(d_0)$ means the maximum displaced distance for all nodes in the first application of the elastic beam algorithm, E_0 is obtained by setting E as an arbitrary value ($E_0 > 0$) in the first application of the elastic beam algorithm, and here $E_0 = 10$.

(2) The iterative process

The elastic beam algorithm is applied iteratively to the proximity graph (G) to compute the displacement for each node in G until a stop condition is reached. The stop conditions are defined as follows.

- **Condition 1:** The iterative process stops if a result that satisfies the defined constraints in *Section 2.1* is obtained after the displacement. Satisfying these constraints means the nodes don't need to be displaced and can be ruled by setting a threshold for the $\max(f_k)$. If $\max(f_k) \leq \varepsilon$, then the iterative process stops; ε is a small constant, i.e., $\varepsilon = 0.001$.
- **Condition 2:** The iterative process stops if a maximum step (T_s) is reached.

Because not all topology relations or contiguities can be maintained, some attractive forces will be redundant. The circles are attracted to be close to each other as much as possible with the applied attractive forces after a set maximum step (Ts') is reached. Thus, if the Ts' is reached and a satisfactory result cannot be obtained, the attractive

forces are not considered in later iterative steps. The iterative process is implemented as **Algorithm 3**, described in Table 3.

Table 3. The iterative process for circle displacement using the elastic beam algorithm.

Algorithm 3. The iterative process for circle displacement

Input: the regions $regS = \{reg_1, reg_2, \dots, reg_m, \dots\}$, their represented circles $CS = \{C_1, C_2, \dots, C_m, \dots\}$, the maximum step for the iterative process is T_s , and the maximum step without considering the attractive forces is T_s'

Output: The $CS = \{C_1, C_2, \dots, C_m, \dots\}$ after displacement

Initialize the iterative step, $t \leftarrow 1$

Do

Construction of the proximity graph (G)

If $t \leq T_s'$ **Then** force computation with attractive forces

Else Then force computation without attractive forces

Compute the displacement vector for each node in G with the elastic beam algorithm, with the maximum force as $\max(f_k)$;

Update the coordinates of each $C_m \in CS$ based on the displacement vector

$t \leftarrow t + 1$

While ($\max(f_k) \leq \varepsilon$ AND $t \leq T_s$)

Return: $CS = \{C_1, C_2, \dots, C_m, \dots\}$

4. Experiments

4.1 Implement details and results

(1) Datasets

Two datasets are taken as experimental data which have been widely used as benchmark datasets for circular cartogram production (Protovis, 2010). (1) Dataset A: The population of 48 states of the United States of America (USA) excluding Alaska and Hawaii in 2015, data source at: <https://hub.arcgis.com/>; (2) Dataset B: The population of each country of North and South America in 2021, data source at: <https://www.unfpa.org/data/world-population-dashboard>.

(2) Parameter settings

Parameters are set as follows: R_{\min} in Eq. (3) is set as 0.1 mm according to the minimum resolution of human eyes, and 0.1mm is a graphic distance(He and Song, 2015); the T_s for the iterative process of the elastic beam algorithm in *Section 3.4* are set by considering the number of the circles ($NumC$) according to Liu et al. (2014), as

follows: $T_s = 4 * NumC$, $T'_s = 2 * NumC$; and if $NumC < 10$, $NumC = 10$.

(3) Experimental environments

We use C# code to implement our proposed approach based on ArcEngine 10.2, and the experiments are carried out on a personal computer with an Intel® Core™ 1.60 GHz i5-8265U CPU and 8G RAM.

Two circular cartograms for the two datasets are successfully generated by using the proposed approach, as shown in Figs. 5 and 6.

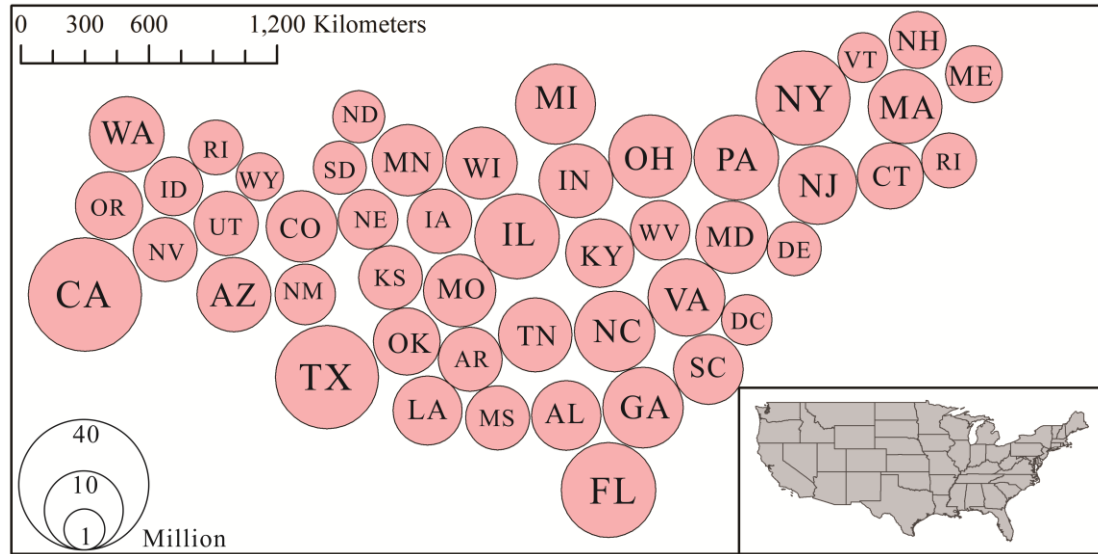


Figure 5. The circular cartogram generated using the proposed approach for the population of each state in the United States of America (excluding Alaska and Hawaii).

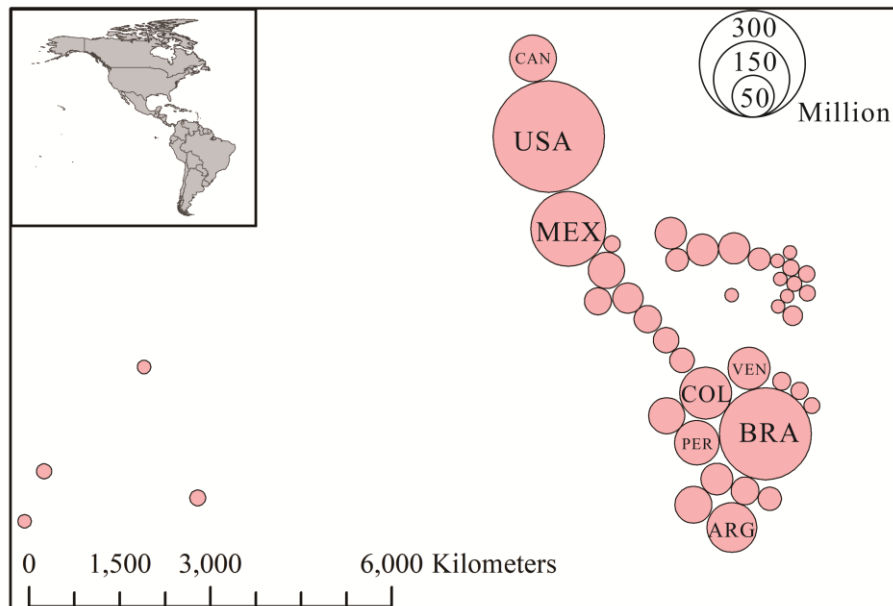


Figure 6. The circular cartogram generated using the proposed approach for the population of each country in North and South America.

4.2 Evaluation and comparisons

(1) Evaluation

The effectiveness of the proposed approach is evaluated by the following measures according to the quality requirements as described in *Section 2.1*: (1) The number of overlaps (*NumO*) evaluates the avoidance of overlaps; (2) The ratio to maintain the adjacent relations (*RT*) evaluates the maintenance of topology relations and contiguities; (3) The root mean square (*RMS*), which describes the variation of direction angles for the links between the centers of neighboring circles evaluates the maintenance of relative relations (Inoue, 2011), and in which two circles connected by an edge in the constructed proximity graph are considered as being neighbors; (4) The total displacement distance (*TDD*) evaluates the minimization of total displacement distance, and *TDD* is computed based on geographic distance. The statistical results are shown in Table 4. From Figs. 5 and 6 and Table 4, we have the following observations: (1) The regions are represented by circles with their sizes in proportion to the populations in the two circular cartograms; (2) No overlaps are generated in the two circular cartograms, which indicates that the proposed approach can avoid overlaps; (3) The *RT* is 68.81% for Dataset A and 71.80% for Dataset B, which indicates that the topology relations and contiguities between regions are mostly maintained; (4) The *RMS* is 24.49 for Dataset A and 24.65 for Dataset B, which indicates that the variations of the relative relations between circles are controlled to a low level. Based on the above observations, we can conclude that satisfactory circular cartograms can be obtained using the proposed approach.

Table 4. Statistical results on the effectiveness of the generated circular cartograms using the proposed approach or Dorling's (1996) approach.

	The proposed approach		Dorling's (1996) approach	
	Dataset A	Dataset B	Dataset A	Dataset B
<i>NumO</i> ↓	0	0	0	0
<i>RT</i> ↑	75/109 = 68.81%	28/39 = 71.80%	70/109 = 64.22%	26/39 = 66.67%
<i>RMS</i> ↓	24.49	24.65	26.16	25.46
<i>TDD</i> (10 ⁶ m) ↓	229.47	204.92	303.30	214.31

The efficiency of the proposed approach is evaluated by using time consumption

(t), as shown in Table 5. It will cost 33.68s to create a circular cartogram for Dataset A and 18.47s to create a circular cartogram for Dataset B. The number of circles (CN) and the number of edges (EN) in the built proximity graph along with the iterative steps (IS) are the key factors that will influence the efficiency, the statistical results are shown in Table 5. By comparing Dataset A and Dataset B, we can see that the larger the CN , EN , and IS , the larger the time consumption. The time consumption will increase if more circles or edges are involved in the circular cartogram production. In most cartograms, however, the number of circles won't be very large by considering the capacity of the map. As shown in Table 5, a circular cartogram with 49 circles and 114 edges will cost 33.68s, this level of efficiency may be acceptable for most circular cartograms.

Table 5. Statistical results on the efficiency of the generated circular cartograms using the proposed approach.

	CN	EN	IS	$t(s) \downarrow$
Dataset A	49	114	98+29	33.68
Dataset B	43	69	86+19	18.47

(2) Comparisons

To validate the feasibility of the proposed approach, we compared it with Dorling's (1996) approach. Results are shown in Fig. 7 and Table 4. From Table 4, we have the following observations: (1) No overlaps are generated using the two approaches, which indicates that both approaches can avoid overlaps; (2) The RT is 4.59% higher for Dataset A and 5.13% higher for Dataset B in comparing the proposed approach to Dorling's approach, which indicates that more adjacent relations between regions can be maintained with the proposed approach. (3) The RMS is 1.67 less for Dataset A and 0.81 less for Dataset B using the proposed approach in comparison with Dorling's approach, which indicates that the proposed approach can better maintain the relative relations between regions. (4) The TDD is 78.83×10^6 m smaller for Dataset A and 9.39×10^6 m smaller for Dataset B in comparing the proposed approach with Dorling's approach, which indicates that the proposed approach has a smaller displacement distance. Based on the above observations, we can conclude that the proposed approach

better maintains the topology relations, relative relations, and contiguities between regions, with smaller displacement distances, in comparison to Dorling's approach.

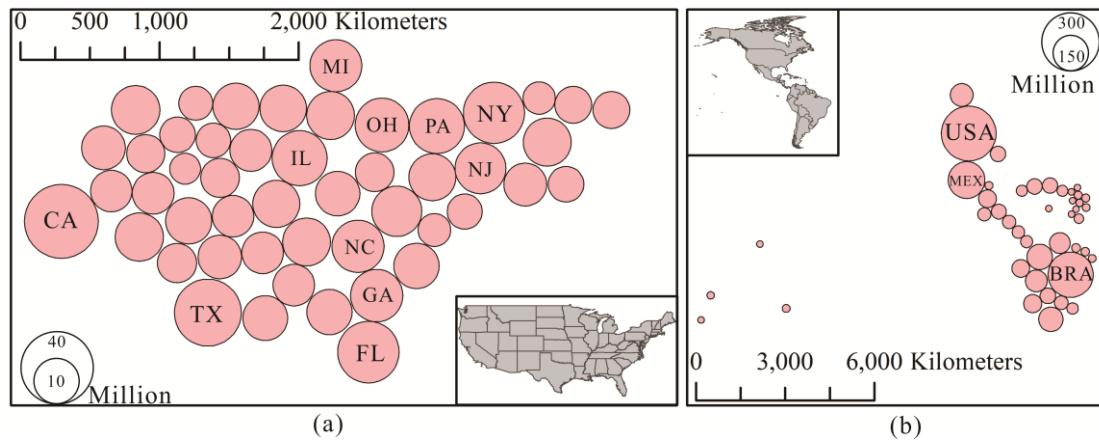


Figure 7. The two circular cartograms generated using Dorling's approach. (a) The circular cartogram for the population of each state in the USA (excluding Alaska and Hawaii); (b) The circular cartogram for the population of each country in North and South America.

4.3 Analysis

The proximity graph construction is the key to consider the quality requirements in our proposed approach. In practice, the quality requirements may vary when considering different user demands. Different proximity graphs may be built and different circular cartograms are then produced. First, the users may decide which edges need to be considered; for example, the users may set a threshold for the edge length or want all circles in the cartogram to be connected as a group. Second, the users may decide which kind of specific proximity graph is to be used, such as a Gabriel graph (GG), relative neighbor graph (RNG), minimum spanning tree (MST), or nearest neighbor graph (NNG) (Wei et al., 2018). Because user demands are diverse, we here analyze two strategies for proximity graph construction: (1) adding restrictions on the long edges, and (2) applying a specific proximity graph.

(1) Restrictions on the long edges

Two circles connected by a long edge may not be visually close to each other (Wei et al., 2018). Furthermore, a large displacement is required to maintain the topology relation or contiguity between their represented two regions. Thus, some users may add restrictions on the long edges, as follows: if two circles are connected by a long edge,

they will not have attractive forces to each other. The long edges are defined by giving a threshold (T_l) for the edge length (L), and T_l is set by the users. If any edge in G satisfies $L > T_l$, then the edge is long.

Fig. 8 gives two example circular cartograms by setting a T_l as 2cm and a T_l as 0cm, T_l is a graphic distance. According to the previous analysis, the T_l is set to avoid large displacements for maintenance of the topology relations and contiguities between regions. Thus, the larger the T_l , the more the maintenance of topology relations and contiguities between regions is considered. When $T_l = 0$ cm, maintenance of topology relations and contiguities between regions are not considered. The statistical results for the two experiments in Table 6 also proves the above analysis, and the displacement distance (TDD) in Table 6 is a geographic distance. As shown in Table 6, setting $T_l = 0$ cm yields a smaller TDD (28.10×10^6 m), RMS (16.01), and RT (29.4%); the TDD increases to 78.35×10^6 m, the RMS increases to 24.56, and the RT increases to 54.13% with $T_l = 2$ cm. But the two circular cartograms have no overlaps with different T_l values, which indicates that satisfactory results can also be obtained by adding restrictions on the long edges.

Table 6. Statistical results on the effectiveness of the circular cartograms by setting different T_l .

	$NumO \downarrow$	$RT \uparrow$	$RMS \downarrow$	$TDD (10^6 \text{ m}) \downarrow$
Cartogram 8(a)	0	32/109 = 29.4%	16.01	28.10
Cartogram 8(b)	0	59/109 = 54.13%	24.56	78.35

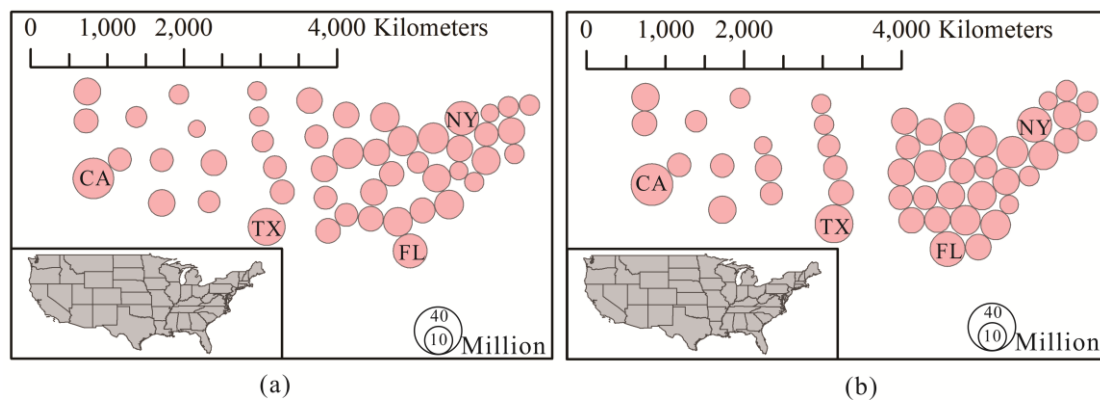


Figure 8. The two circular cartograms generated by using the proposed approach with different T_l

for the population of each state in the United States of America (excluding Alaska and Hawaii). (a) $T_l = 0\text{cm}$; (b) $T_l = 2\text{cm}$.

(2) Application of a specific proximity graph

Different proximity graphs have been defined in the geographic information science (GIS) domain to represent different kinds of proximity relations, such as GG, RNG, MST, and NNG (Wei et al., 2018). These proximity graphs can also be applied for circular cartogram production according to specific user demands. Fig. 9 gives two example circular cartograms using the proposed approach, in which the MST is taken as the proximity graph. Because the overlaps must be avoided in a circular cartogram, edges are also inserted in the MST if two circles overlap. As shown in Fig. 9, two circular cartograms can be successfully generated with no overlap and maintenance of contiguity. Because the circles are structured by an MST, their arrangements are also MST-like. The MST can further be changed into any other defined proximity graph (G) by users, and a circular cartogram with a G -like arrangement can then be generated. These results indicate that our proposed approach can be applied for arbitrary proximity graphs.

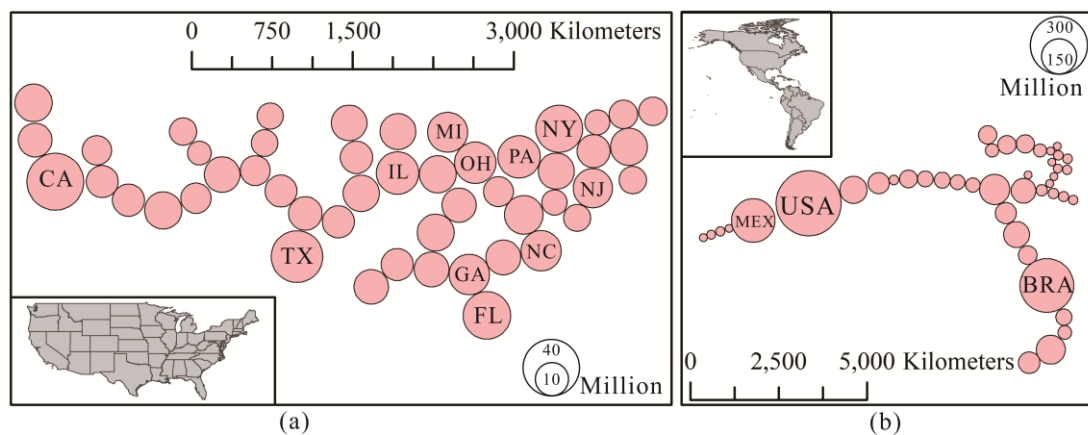


Figure 9. Circular cartograms for two datasets in which proximity graphs are built based on the minimum spanning tree (MST). (a) The circular cartogram for the population of each state in the United States of America (excluding Alaska and Hawaii); (b) The circular cartogram for the population of each country in North and South America.

5. Conclusions

To generate a circular cartogram for quantitative visualization, we apply the elastic beam algorithm that originated in cartographic generalizations for circle displacements. The displacement mechanism is controlled by enforcing the quality constraints for circular cartogram production in the proximity graph construction and the force computation. To avoid huge overlaps and gaps, the initial circles are also generated with an alternative directions and reduced steps algorithm. Experiments show that circular cartograms obtained by the proposed approach have higher quality with respect to the maintenance of topology relations, contiguities, and relative relations with smaller displacement distances. Furthermore, our proposed approach is also applicable for arbitrary proximity graphs by considering varied user demands.

Future work will focus on: (1) Design of animated circular cartograms, which are applicable for time series data; (2) Improvement of algorithm efficiency.

Disclosure statement

No potential conflict of interest was reported by the author(s).

Data and code availability statement and data deposition

The data and code that support the findings of this study are all openly available, website is: <https://github.com/TrentonWei/DorlingMap>

References

- Bader M. (2001) Energy minimization methods for feature displacement in map generalization. Doctorate thesis, Geographic Information System Division, Department of Geography, University of Zurich, Switzerland.
- Buchin K, Speckmann B, Verdonschot S. (2012). Evolution strategies for optimizing rectangular cartograms[C]//International Conference on Geographic Information Science. Springer, Berlin, Heidelberg, 29-42.
- Bostock M., Ogievetsky V., Heer J. (2011). D3 data-driven documents. IEEE Transactions on Visualization and Computer Graphics 17(12): 2301–2309.
- Chrisman, N. R. (1977). Cartogram projections of planar polygon networks. Harvard Laboratory for Computer Graphics and Spatial Analysis, Harvard University.
- Chrisman, N. R. (2002). Exploring geographic information systems (2nd ed.). Wiley.

- D3.js - data-driven documents. <http://d3js.org/>, 2013.
- Dorling D F L. Area cartograms: their use and creation[M]//Concepts and techniques in modern geography series. Environmental Publications, University of East Anglia, 1996.
- Dougenik, J. A., Chrisman, N. R., Niemeyer, D. R. (1985). An algorithm to construct continuous area cartograms. *The Professional Geographer*, 37(1), 75–81.
- Du, C., Liu, L. (1999). Constructing contiguous area cartogram using ArcView avenue. *Proceedings of Geoinformatics '99 Conference*, Ann Arbor, MI.
- Florinsky I. (2016). *Digital terrain analysis in soil science and geology*. Academic Press.
- Fei, L. (2002). A method of automated cartographic displacement: On the relationship between streets and buildings. *Fachrichtung Vermessungswesen der Univ.*
- Gastner M. T., Newman M. E. J. (2004). Diffusion-based method for producing density-equalizing maps[J]. *Proceedings of the National Academy of Sciences*, 101(20): 7499-7504.
- Gastner M T, Seguy V, More P. (2018). Fast flow-based algorithm for creating density-equalizing map projections[J]. *Proceedings of the National Academy of Sciences*, 115(10): E2156-E2164.
- He Z. & Song Y. (2015). *General Map Complilation*[M]. Wuhan:Wuhan University Press.
- Heilmann R., Keim D., Panse C., Sips M. (2004). Recmap: Rectangular map approximations[C]//*IEEE Symposium on Information Visualization*. IEEE, 33-40.
- Inoue R. (2011). A new construction method for circle cartograms[J]. *Cartography and Geographic Information Science*, 38(2): 146-152.
- Jackel, C. B. (1997). Using ArcView to create contiguous and noncontiguous area cartograms. *Cartography and Geographic Information Systems*, 24(2), 101–109.
- Kronenfeld B. J. (2018). Manual construction of continuous cartograms through mesh transformation. *Cartography and Geographic Information Science*, 45(1): 76-94.
- Liu Y, Guo Q, Sun Y, et al. (2014). A combined approach to cartographic displacement for buildings based on skeleton and improved elastic beam algorithm[J]. *PloS one*, 9(12): e113953.

- Nusrat, S., & Kobourov, S. (2016). The state of the art in cartograms. *Computer Graphics Forum*, 35(3): 619-642.
- Protovis – Dorling Cartograms. <http://mbostock.github.io/protovis/ex/cartogram.html>, 2010.
- Raisz E. (1934). The rectangular statistical cartogram. *Geographical Review*. 24(3): 292–296.
- Reyes Nunez J. J. (2014). The use of cartograms in school cartography. *Thematic Cartography for the Society*, 327–339.
- Robinson A. H. (1955). The 1837 maps of Henry Drury Harness. *The Geographical Journal*, 121(4): 440–450.
- Speckmann B., Kreveld M., Florisson S. (2006). A linear programming approach to rectangular cartograms. In *International Symposium on Spatial Data Handling (SDH'06)*.
- Sun, S. (2013a). A fast free-form rubber-sheet algorithm for contiguous area cartograms. *International Journal of Geographic Information Science*, 27(3): 567–593.
- Sun, S. (2013b). An optimized rubber-sheet algorithm for continuous area cartograms. *The Professional Geographer*, 65(1): 16–30.
- Sun S. (2020). Applying forces to generate cartograms: a fast and flexible transformation framework. *Cartography and Geographic Information Science*, 47(5): 381-399.
- Tang W. Parallel construction of large circular cartograms using graphics processing units[J]. *International Journal of Geographical Information Science*, 2013, 27(11): 2182-2206.
- Tobler W. (2004). Thirty five years of computer cartograms[J]. *ANNALS of the Association of American Geographers*, 94(1): 58-73.
- Van kreveld M., Speckmann B. (2005). Rectangular cartogram computation with sea regions. In *Proc. 22st Int. Cartographic Conference*.
- Van kreveld M., Speckmann B. (2007). On rectangular cartograms. *Computational Geometry*, 37(3):175–187.
- Wei Z., Guo Q., Wang L., F. Yan. (2018). On the spatial distribution of buildings for

map generalization. *Cartography and Geographic Information Science*, 45(6): 539-555.

Wolf, E. B. (2005). Creating contiguous cartograms in ArcGIS 9. Proceedings of 2005 ESRI International User Conference, San Diego, CA.